SPE 115732

Mechanisms of Meniscus Motion in Fractionally Wetted Porous Media

Siyavash Motealleh, SPE, Mandana Ashouripashaki, SPE, David DiCarlo, SPE, and Steven Bryant, SPE,
The University of Texas at Austin

This paper was prepared for presentation at the 2008 SPE Annual Technical Conference and Exhibition held in Denver, Colorado, USA, 21–24 September 2008.

Abstract

Oil reservoirs and soil are often heterogeneously wetted (mixed wettability or fractional wettability). In mixed-wet reservoirs the mechanism of wettability alteration means that a single grain can have patches that are water-wet and patches that are oil-wet. In fractionally-wet porous media each grain is either oil-wet or water-wet. Here we develop a mechanistic model of capillarity-controlled fluid movement in fractionally-wet media. The model calculates the position of stable interfaces between grains of arbitrary wettability. Pore filling occurs when the interface becomes unstable in a pore throat (Haines condition), or when two or more interfaces come into contact and merge to form a single interface (Melrose condition). The model is robust and general in the sense that both filling mechanisms are considered simultaneously during arbitrary sequences of changes in capillary pressure. The model is demonstrated on 2-D porous media consisting of randomly distributed oil-wet and water-wet disks, and capillary pressure – saturation curves are obtained. The model results compare favorably with imbibition experiments on fractionally-wet media. Most notably, a distinctive shift in the drainage/imbibition curves occurs as the fraction of oil-wet grains increases beyond a threshold value.

Introduction

In a rock containing immiscible fluids, the rock is wetted by the fluid that has smaller surface energy of interaction with the rock (Dullien 1992). Wettability of reservoir rocks is the subject of wide investigation because understanding rock wettability helps petrophysicists to estimate fluid distribution within the pore space of the rock (Anderson 1987a and 1987b). Fluid distribution at the pore scale is important because this affects the macroscopic rock/fluid properties such as capillary pressure curves and relative permeability curves.

Many rock minerals have a tendency to be wetted by water and thus, reservoir rocks are typically water-wet before they are filled with oil. However, chemical species within the oil that are charged can change the wettability of the reservoir rocks to oil-wet during geological time (Salathiel 1973). Reservoirs can be partly oil-wet and partly water-wet due to wettability alteration, which occurs on the part of the reservoir rock that is exposed to the crude oil (Salathiel, 1973). This is referred to in the literature collectively as heterogeneous wettability (Laroche *et al*. 1999), fractional wettability (Tsakiroglou and Fleury 1999), and mixed wettability (Al-Futaisia and Patzek 2004, Valvatne and Blunt 2004, Piri and Blunt 2002, van Dijke *et al*. 2000).

Here, we identify two categories of heterogeneous wettability: fractional wettability and mixed wettability. In the case of fractional wettability the grains that construct the porous medium are either water-wet or oil-wet. The water-wet and oil-wet grains are distributed randomly within the porous medium. This is depicted schematically in Fig. 1.

In the laboratory, the fractionally wetted porous media are prepared by mixing different fraction of the oil-wet grains and water-wet grains. Fractionally wetted porous media occur naturally in certain soils, and they are the simplest heterogeneously wet media that can be reliably reproduced experimentally. Because of this fractionally wet media has been the focus of most experimental measurements (Ustohal *et al*. 1998, Han *et al*. 2006, Bradford and Leij 1995, Bautersa *et al*. 2000, Sharma *et al*. 1991).

In contrast for mixed wet porous medium, the grains may have both water-wet and oil-wet patches. This can occur from different mineral surfaces on the grain (micas or quartz), or it may occur from different portion of the grains coming in contact with reservoir oil. In nature, oil invades the water-wet rock due to density differences between oil and water (first migration). During first migration water is displaced from large pores, and remains in both small pores and as rings at the grain contacts due to capillary force. It is theorized that wettability alteration occurs only on the surfaces of grains that directly contact the oil phase; therefore the surfaces of the grains within the small pores, which were never filled with oil,

remain water wet. Similarly, the surfaces of the grains where the pendular ring forms remain water wet (Fig. 2). This mechanism of wettability alteration causes single grains to have both water-wet and oil-wet patches (Salathiel 1973).

Brown and Fatt (1956) were the first to construct heterogeneously wetted porous media. They mixed different fraction of oil-wet and water-wet sand grains to build several fractionally wetted porous media. The authors showed that "wettability" of the model rock could be measured by Nuclear Magnetic Relaxation method (NMR).

McDougall and Sorbie (1993) investigated waterflood performance in heterogeneously wetted porous media. They modeled mixed-wet rock as porous media composed of small pores (water-wet) and big pores (oil-wet). They also modeled fractionally wetted porous media by choosing certain fractions of pores water-wet and oil-wet, independent of the pore sizes. They use the invasion percolation theory to model the capillary displacement of water and oil phase. Other researchers (Blunt 1998, Piri and Blunt 2002, Mohanty and Salter 1983, Heiba *et al*. 1983) have studied the mixed wet and fractionally wetted porous medium using pore network modeling. Their pore network models are typically based on a lattice of random pores and throats with different shape (triangular, square, circular, star-shape, etc). The shapes are inspired by naturally occurring throats, which retain wetting phase at grain contacts after the throat has drained. By retaining wetting phase in the corners the shaped throats represent a useful advance over traditional cylindrical throats. However, a concept not considered in the above models is that 'pore is the space where grains do not exist'. In other words, the pore shapes are not fundamental; rather, the grain shapes are the "primitives" from which pore shapes are derived. Moreover, wettability is strictly speaking a property of grains, not of pores. A grain-based approach to this class of fluid displacements therefore seems natural.

The essential features of a grain-based approach are (i) the locations of the grains and (ii) the wettability (contact angle) of each grain. The former data allow an unambiguous identification of pores and throats, without recourse to sampling a distribution or specifying a shape. The latter data lead to criteria for stable configurations of a meniscus. The fundamental event in a grain-based approach is the filling of an individual pore, just as in traditional pore network models. However we establish criteria for such events in terms of grain locations and contact angles, rather than in terms of the geometry of idealized throats. For invasion of a pore by a single meniscus passing through a throat, the grain-based and pore network models arrive at essentially the same result, namely the criterion for a Haines jump. For invasion of a pore by the merger of two (or more) interfaces, the grain-based approach offers a significant advantage. The correct geometry and location of pendular rings (at contacts between pairs of grains) and of menisci (between three or more grains) are readily determined in a grain-based model. We are unaware of any systematic way to account for these phenomena in a pore network model. Haines jumps and Melrose mergers both occur during any cycle of drainage or imbibition in a fractionally wet medium. We conclude that a grain-based approach is essential for obtaining a mechanistic understanding of such displacements. This assertion is supported by the successful prediction of imbibition curves in uniformly wetted media (Gladkikh and Bryant 2005).

An example of the grain-based approach is found in Ustohal *et al*. (1998), who study the hydraulic characteristics of fractionally wetted porous media. They develop the criteria for movement of menisci using a capillary tube as an idealized pore. They apply those criteria to their porous media (clusters of grains).

This paper is part of a broader effort to understand the mechanisms of meniscus movement in heterogeneously wet media, then to use that understanding to develop purely mechanistic and geometric criteria for pore level events. We need to validate our simulation result (drainage and imbibition curves), and hence the geometric criteria on which the simulation relies, against experimental data. The criteria applied in fractionally wetted porous media are not fundamentally different from criteria applied in mixed wet porous media. The experimental data for fractionally wetted media are more readily available due to the simplicity of the experimental set up. The comparison between experimental data and simulation result is also easier in fractionally wet media because independent variable is simply the percentages of oil-wet and water wet grains. In contrast in a mixed-wet porous medium the configuration of oil wet and water wet surfaces (wettability map) is very complicated, depending on pore geometry, the history of primary drainage, etc. For the purpose of validating mechanisms, then, the fractionally wet medium is preferred.

We restrict ourselves to two-dimensional media in this paper. This greatly simplifies the presentation and implementation of the concepts. The extension to three dimensions is straightforward but tedious.

Terminology

Because the solid surfaces in a heterogeneously wetted porous medium consist of surfaces with different wettability, discrimination between wetting and non-wetting phase is ambiguous. Hence we define capillary pressure to be the pressure of the non-aqueous phase (oil) minus pressure of the aqueous phase (water or brine).

$$P_c = P_o - P_w \tag{1}$$

This macroscopic capillary pressure is proportional to the curvature of the microscopic interfaces through the young Laplace equation,

$$P_c = \sigma_{ow}\left(\frac{1}{r_1} + \frac{1}{r_2}\right) = 2C\sigma_{ow} \tag{2}$$

where r_1, r_2 are radii of curvature and C is defined as the mean curvature. The curvature is essentially a scaled capillary pressure. Thus when the pressure of oil phase exceeds the water phase pressure, the capillary pressure and curvature are positive and consequently the interface curves toward the oil phase, and when the capillary pressure and curvature are negative the interface curves toward the water phase. These curved interfaces are referred to as menisci.

Along these lines and following Morrow (1990), we define drainage to be when the water saturation is decreasing, and imbibition to be when the water saturation is increasing.

Model/Simulation

Haines Events. Pores can fill through two different mechanisms, Haines events (Haines 1927) and Melrose events (Melrose 1965). These can be most easily understood in uniformly water wet media. Figure 3 shows a schematic of a Haines event. As the capillary pressure increases, the curvature increases, and the meniscus gradually moves to the right into ever narrower parts of the throat. At location 3 the throat can no longer hold the meniscus, and it jumps to displace the fluid from the pore behind the throat. The criterion for this 2D Haines event is given by the smallest circle that will fit in the throat; for curvatures greater than this curvature, the meniscus will pass through the throat.

Melrose Events. A Melrose event is the irreversible jump that occurs after two separate menisci come into contact and merge into a single meniscus. Figure 4 shows a Melrose event in a uniformly water-wet medium during imbibition (curvature decreasing). The details are as follows. The decrease in the curvature causes advancement of the menisci from the upper and lower throats on the right (location 1) toward the pore (locations 2 and 3). Continued advancement results in the merging of menisci at location 3 to form a single meniscus. This configuration is not stable. Upon an infinitesimal decrease in curvature, the wetting phase fills the pore space completely and makes a new meniscus in the throat of neighboring pores, location 4. Thus the criterion for a Melrose event is the touching of two separate interfaces. For a pore with multiple throats, several different Melrose events are theoretically possible, depending on which pairs of throats contain the merging menisci.

Figures 3 and 4 also illustrate the geometric cause of hysteresis in a drainage and imbibition cycle. The critical location of the meniscus during drainage (location 3 in Fig. 3) is quite different from the critical location during imbibiton (location 3 in Fig. 4). Hence the curvature (and capillary pressure) at which each event occurs is quite different.

Shape of Water/Oil Interface (Meniscus) on the Fractionally Wetted Throat. In the fractionally wetted porous medium the configuration of the oil-wet and water-wet surface dictates the fluid distribution within porous medium. Within a two-dimensional network of disks three neighboring disks construct a pore and each pore has three throats constructed from pairs of adjacent disks (Fig. 5). There are four configurations of grains defining a pore in the fractionally wetted porous medium:

- Three water-wet disks, in which all throats are water-wet. (Fig. 5a)
- Three oil-wet disks, in which all throats are oil-wet. (Fig. 5b)
- Two water-wet disks and one oil-wet disk, in which one water-wet and two fractionally wetted throats. (Fig. 5c)
- Two oil-wet disks and one water-wet disk, in which one oil-wet and two fractionally wetted throats. (Fig. 5d)

The task is to determine the Haines and Melrose events that can occur in each type of pore. This reduces to two more basic exercises: computing the critical curvature for a single meniscus in a throat, and computing the critical curvature for two menisci in adjacent throats. The solution to the first exercise, which we summarize next, is the foundation for the second. We treat curvature (or capillary pressure) as the independent variable. This is driven by the common experimental procedure of incrementing capillary pressure, waiting for equilibrium and repeating. To determine when Melrose and/or Haines criteria are met in the corresponding simulation, it is necessary to calculate the position of all of the menisci within the porous medium at a prescribed curvature.

Stability of Meniscus in Fractionally Wetted Throat, Analogy to Haines Criterion. We generalize the classical Haines criterion by solving for the stable interface in fractionally-wet media. Here we demonstrate how the position of one meniscus is found between a pair of 2-D discs of arbitrary and unequal contact angles and radii, separated by an arbitrary gap D, Fig. 6.

For a meniscus with constant curvature, the geometry of the meniscus is defined by the center of the curvature (x_0, y_0), the radius of curvature, and the intersections with the solid surface. The intersections of the meniscus with the discs are forced to be at the contact angle of each surface. These constraints yield a trigonometry problem to be solved for the center of curvature. Figure 6 shows the schematic of menisci positioned on the two disks with different contact angles (θ_1, θ_2).

In the configuration of Fig. 6, R_1, R_2 (radii of disk 1 and 2), contact angles (θ_1, θ_2), the gap D, and the radius of the meniscus r are given. A solution for the center of the meniscus exists if the following condition is met.

$$\frac{(D+R_1+R_2)^2-(L_1-L_2)^2}{2L_1L_2} \le 2 \tag{3}$$

where L_1 and L_2 are the distances from the center of each disk to the center of meniscus and are given by

$$L_1 = \sqrt{R_1^2 + r^2 + 2R_1 r\cos(\theta_1)} \tag{4}$$

$$L_2 = \sqrt{R_2^2 + r^2 + 2R_2 r\cos(\theta_2)} \tag{5}$$

If equation 3 is met, the interface can exist between the grains, and the interface is stable. If it is not met, the interface cannot exist. Thus equation 3 implies a critical value of curvature, namely the largest value for which the interface is stable. As shown empirically above, this critical curvature is one for which the interface will first pass through the throat. If the interface is stable and the curvature is changed such that the condition is no longer satisfied, the interface will pass through this throat in a Haines event.

Equation 3 is a general criterion for any two disks with different contact angles and different radii. We illustrate it for two specific cases that are frequent in the fractionally wet medium

Figure 7 show the schematic of a meniscus positioned on two disks of equal size with zero contact angles ($\theta_1=\theta_2=0$).

In Fig. 7 the distances from center of each disk to the center of meniscus are equal:

$$L_1 = L_2 = r + R \tag{6}$$

Substituting equation 6 in equation 3 reduces the criteria of stable meniscus to

$$r \geq \frac{D}{2} \tag{7}$$

Equation 7 defines a minimum radius of curvature stable for given gap *D*. It is instructive to rewrite Equation 7 in terms of curvature, yielding a criterion for the maximum curvature (capillary pressure) allowable for the meniscus to be stable:

$$C \leq \frac{2}{D} \tag{8}$$

Thus as soon as the curvature of the meniscus exceeds the critical value of $D/2$, the radius of the meniscus becomes smaller than half of gap size, the position of the meniscus becomes unstable, and a Haines' jump occurs. This curvature is the Haines criteria for this throat.

The other specific case of interest is when two disks have the same radii and opposite wetting preference. Figure 8 shows the schematic of a meniscus positioned on two disks of equal size with 0^o and 180^o contact angles ($\theta_1=0^o$, $\theta_2=180°$).

Regarding Fig. 8, we can observe that

$$L_1 = r + R, \quad L_2 = r - R \tag{9}$$

Substituting equation 4 into equation 1 leads to

$$r \geq \frac{D}{2} + R \tag{10}$$

Typical values of *D* are three to ten times smaller than *R*. Thus comparing equation 10 to equation 6 shows that the minimum radius of curvature is much larger if one of disks is oil-wet (contact angle equals to 180^o). This means that the maximum value of curvature for a stable meniscus is much smaller when one disk is oil-wet. So the meniscus will become unstable in such a throat at a relatively small value of curvature, while menisci in water-wet throats remain stable. Thus, in a large collection of oil-wet and water-wet disks, the range of curvatures for which menisci are stable in all the throats in the domain is very small. This statement is true for positive applied curvature.

Stability of Two Merging Menisci in Fractionally Wet Media, Analogy to Melrose Criterion. The Haines criterion obtained above applies to a single meniscus between a pair of grains. We now consider two menisci at adjacent throats in a single pore. To understand the Melrose event geometrically, first consider a uniformly wetted pore, shown in Fig. 9. The pore has three uniformly wetted throats. Originally two menisci are located at adjacent throats (Fig. 9a). Decreasing the curvature causes the menisci to move toward the pore (i.e. to the right) (Fig. 9b). The angle α subtended by the points of contact of the menisci on the center grain decreases as curvature decreases. The moment the menisci touch, i.e. when $\alpha = 0$, they become

unstable and merge into one meniscus. They leave the center disk so the pore will be filled with water (Fig. 9c). This series of events occurs during an imbibition process as the curvature and capillary pressure are decreased.

The same kind of event (merging two menisci) can occur by increasing curvature in a fractionally wetted pore (Fig. 10). In Fig. 10 we show a single pore made up of two water-wet disks and one oil-wet disk. The pore has one uniformly wetted throat and two fractionally wetted throats. Originally two menisci are located at adjacent fractionally wet throats (Fig. 10a). This time they move toward the pore as curvature increases (Fig. 10b). The moment they touch they get unstable and merge to one meniscus, (Fig. 10c). These series of event occurs in drainage process as the curvature and capillary pressure are increased.

Grain-based Displacement Model

To study the movement in menisci through fractionally wet porous media, we create 2-D porous media made up of equally sized disks. The disks cannot overlap but otherwise are randomly located. Each disk can be made either water or oil-wet.

To facilitate movement of water and oil through the network we also create an oil-wet membrane made of smaller sized oil-wet disks on the left hand side, and a similar water-wet membrane on the right hand side of the model (Fig. 11a).

We use a Delaunay tessellation of the disks centers to subdivide the pore space into pore bodies and pore throats. The tessellation yields triangles, with each face of the triangle corresponding to a pore throat. The space inside each triangle (excluding the disks) is the pore body (Fig. 11b).

With this means of identifying pores, it is possible to simulate drainage and imbibition process by applying the criteria developed above to each pore throat and pore body in the domain. We simulate the menisci motion using the invasion percolation algorithm, changing curvature in small increments then computing the stable meniscus locations in all pores. At any given curvature (capillary pressure) all pores that are connected to the outlet will be in candidate list for invasion. We check the candidate pores for criteria of invasion (Melrose or Haines criteria). If a candidate meets the criteria of invasion and it also connected to the outlet, we invade the candidate and add the neighboring pores to list of candidate, we continue until there is no candidate remains in the list. Candidates that are not connected to the outlet are labeled “trapped” and removed from further consideration of events. Then we increase or decrease the curvature incrementally and we repeat the procedure.

Results

Figure 12 shows the imbibition and drainage curves for a porous medium with 50% of disks are oil-wet. For this and subsequent figures, the curvature is normalized such that a curvature of 1 corresponds to the radius of the disks. Initially the porous medium was filled with oil (Fig. 12, point P0), so the first process is primary imbibition where the water phase imbibes to the porous medium until residual oil phase saturation. Then drainage process starts from imbibition end point (Fig. 12, point P1) with increasing capillary pressure and increasing water saturation. Finally the secondary imbibition starts from drainage endpoint (Fig. 12, point P2) and imbibe to porous medium to new value of residual oil phase saturation (Fig.12, point P3). The model allows seamless movements of interfaces and filling events even through the zero capillary pressure level. Both Haines and Melrose events can occur with a change in the capillary pressure. All menisci are tested for both types of events depending on their local circumstances. Thus the critical curvature for local events is dynamic and cannot be pre-calculated. This is unlike traditional invasion percolation models.

Figure 13 shows the fluid configuration corresponding to point (P2) at the drainage curve in Fig. 12. One can see the water trapped inside the porous medium in disconnected blobs. From the figure, the edges of the blobs typically consist of a boundary “shell” of water-wet grains surrounded by another shell of oil-wet grains.

This modeling approach considers both Haines and Melrose events on imbibition and drainage, as is necessary for mixed-wet or fractionally-wet media. This gives the model an inherent robustness in the sense that all grains, throats, and pore bodies are considered equivalent, just with a different contact angle for each grain. This robustness can be seen by considering a 25% oil-wet medium, and the equivalent 75% oil-wet medium in which all of the oil-wet grains are made water-wet and vice-versa. By reversing the wettability of each grain, the capillary pressure curve should also reverse. Figure 14a shows the 25% oil-wet capillary pressure curve obtained with the model, and Fig. 14b shows the 75% oil-wet capillary pressure curve. The symmetry is evident, as the drainage in the 25% oil-wet medium is identical to the imbibition in the 75% water-wet medium. This shows that the model is performing as expected.

Note that this symmetry is only seen if each grain’s wettability is reversed. If the position of the grains is different, or the pattern of the oil-wet grains is different, the model will show slightly different capillary pressure curves.

We emphasize that by checking Haines and Melrose criteria for all pores, the algorithm has generalized the notion of simulating drainage and imbibition. The very same code is used for all paths shown in Fig 14; the only difference inside the code between drainage and imbibition is the sign of the increment in curvature. In contrast, traditional pore network models have algorithms specific to drainage and different algorithms for imbibition; only the machinery of invasion percolation is common to both. Applied to uniformly wetted media, our algorithm correctly finds only Haines events during drainage and only Melrose events during imbibition.

We can now use the model to study how the drainage and imbibition curves vary with the change of oil-wet fraction. Figure 15 shows the primary drainage curves for porous media with different fraction of oil wet disks. As before, the oil-wet disks have a contact angle of 180° and the water-wet disks have a contact angle of 0. As expected, with increasing oil-wet fraction in the media, the drainage curves move to lower capillary pressures. What is interesting is in the fact, that the

movement is not linear. Small (10%, 20%) percentages of the oil-wet fraction do not significantly change the position of the drainage curve from the complete water-wet case. Large changes in the curve are only seen once a threshold of approximately 40% oil-wet grains is achieved. Likewise, when the medium is primarily oil-wet (> 80%), the changes in the drainage curve are minor.

Figure 16 shows the model results for the primary imbibition curves for porous media with different fraction of oil wet disks. Again, the curves tend to lower capillary pressures with increasing oil-wet fraction. Also again, the change in capillary pressure is minor for the first 20-30% of oil-wet grains, the change is large for oil-wet percentages around 50%, and the change is small when the oil-wet fraction is greater than 70-80%.

Experiment

We performed laboratory experiments to obtain water/air pressure-saturation curves for primary drainage, primary imbibition, and secondary imbibition into fractionally-wet sand packs. A water-wet sand (grain size d_{50} = 15μm) was used as the water-wet grains; the oil-wet grains were made by tumbling the clean sand in a 5% OTS (octatrichlorosilane) in ethanol solution for 5 hours. After tumbling, the sand grains were rinsed in ethanol 5-6 times to remove the excess OTS, followed by air drying the sand. Fractionally-wet packs were made by mixing prescribed proportions of the water-wet and oil-wet grains.

The experiments were performed in 60 cm long columns (2.54 cm inner diameter), which were filled with the fractionally-wet sand. The columns consisted of separate 3 and 1 cm long sections of polycarbonate tubing that were held together with polyolefin shrink tubing. For drainage, the column was filled from below with water and flushed for 1 hour to remove entrapped air. Primary drainage was then performed by attaching a constant head tank to the outlet at the bottom of the column, and air was allowed to enter the top at atmospheric pressure. Primary imbition starts with an air-dry column, and the attachment of the constant head tank at the bottom of the column. For imbibition, the height of the constant tank was chosen such that the water would rise roughly halfway through the column. Each column was allowed to equilibrate for 1 week. After this, the capillary pressure in each section was obtained assuming capillary gravity equilibrium. The water content was obtained by sectioning the column, and obtaining the water saturation through the section's wet and dry weight.

Figure 17 shows the measured P-S curves for primary drainage for 5 different sands of varying oil-wet fraction, and Fig. 18 shows the P-S imbibition curves. The open symbols are the measured data for each oil-wet fraction. The lines are Corey type fits to the data first used by Skjaeveland *et al*. (2000) and are explained as follows. The 0% oil-wet data was fit to a standard water-wet Corey P-S curve (P_{cw}),

$$P_{cw} = P_{bw}\left(S_w\right)^{-1/\lambda_w} \tag{11}$$

where P_{bw} is the bubbling pressure for the water wet media, and λ_w is the Corey exponent for the water-wet media. The 100% oil-wet data was fit to an oil-wet Corey P-S curve (P_{co}),

$$P_{co} = P_{bo}\left(S_o\right)^{-1/\lambda_o} \tag{12}$$

where P_{bo} is the bubbling pressure for the oil-wet media (necessarily negative), and λ_w is the Corey exponent for the oil-wet media. For the fractionally-wet data we use a linear combination of the water-wet and oil-wet curves,

$$P_c = \alpha P_{cw} + \left(1-\alpha\right) P_{co} \tag{13}$$

and the curve fitting for these curves is just for the parameter α, that is, the values of λ_w and λ_o are fixed by the 100% water-wet and 100% oil-wet curves. The curve fitting parameters are shown in the table below.

For the experimentally measured drainage curves (Fig. 17), there is very little change for all oil-wet fractions, and the curves remain in the positive capillary pressure region, and thus only the parameters for the water-wet curve are given. For the experimentally measured imbibition curves, there is a monotonic variation from 0% to 100% oil-wet and the parameters are listed in the table.

Figure 18 and Table 1 show how the parameter α varies as a function of oil-wet fraction. Here the non-linear change in pressure-saturation curve as a function of oil-wet fraction is evident, as predicted by the model in Fig. 16. We do not expect quantitative agreement between 2D simulations and 3D experiment, but the qualitative consistency indicates that the theoretical treatment does capture the behavior of menisci in fractionally wet media.

Discussion

The model developed in this paper consists of 2-D discs as it is the simplest to observe the actual mechanics of the menisci movement. Clearly the percolation threshold and the trapped phases will change in a 3-D rather than a 2-D model. Still there

are many parallels between the P-S curves obtained from this 2-D model and those obtained from experiments in 3-D porous media.

The most obvious parallels are seen for the imbibition curves in Figs. 16 (model) and 18 (experiment). When the capillary pressure is increased, the water saturations go from near saturated followed by a jump to completely unsaturated at a specific capillary pressure. This transition capillary pressure decreases monotonically with increasing oil-wet fraction in both figures. More interestingly, the transition capillary pressure does not change linearly with oil-wet fraction in either figure. Looking at the model results (Fig. 16), starting from 0% oil-wet fraction, the transition capillary pressure decreases only slightly up to about 40% oil-wet fraction; between 40% and 60% oil-wet fraction there is a large decrease in the transition capillary pressure; finally between 60% and 100% the transition capillary pressure decreases only slightly. Looking at the experimental results (Fig. 18), the same pattern is observed: a slight change of the transition capillary pressure between 0% and 25% oil-wet fraction; a large change between 25% and 75%, and finally a slight change between 75% and 100%. This can also be seen in Table 1 with the non-linear progression of α with decreasing oil-wet fraction.

The simplest explanation is in terms of percolating clusters of like wettability grains. The model suggests that the capillary pressure curve shows minor changes until 40% of the grains are oil-wet. Above this threshold, there are enough oil-wet grains to percolate across the model, allowing a rapid change in the capillary pressure curve. The experimental data are not obtained for as many fractions as the model, so the exact percentage of oil-wet grains needed to percolate is unknown (it is somewhere between 25% and 50%). It is likely that the 2-D model and 3-D experiments would lead to different percolating fractions, but the general nature of the curves would be similar.

For the drainage curves, the match is not as straightforward, mainly because there is no observed change in the transition capillary pressure for the experiments. Similar experimental behavior was observed for water/air systems with the oil-wet grains being silanized versions of the water-wet grains (Bauters *et al*. 2000, Ustohal *et al*. 1998). In this case, it is most likely a result of the contact angle not being 180° for drainage from the oil-wet grains. Ustohal *et al*. estimates a receding (draining) contact angle of 50° for silanized sand, far from the 180° that the model results in Fig. 15 show. The model is robust enough to handle different contact angles in calculating the movement of the menisci. Figure 19 shows the model results for drainage from fractionally-wet media, where the contact angle of the water-wet grains is 0° and the contact angle of the oil-wet grains is 50°. As in Fig. 15, the transition capillary pressure decreases with increasing oil-wet fraction, but the change in capillary pressure is much less. The fit with the experiments in Fig. 17 is better, suggesting that careful, independent measurement of contact angle is necessary for evaluating behavior of fractionally wet media.

Conclusion

We develop a grain-based, mechanistic model for oil/water displacement under capillary control in fractionally wet media. The model invokes the two types of irreversible pore-level events, Haines jumps (single meniscus in a throat) and Melrose mergers (two menisci in adjacent throats). We implement and illustrate the model in 2D, solving analytically for stable configuration of the meniscus held between pairs of grains of arbitrary and unequal contact angle. We carry out drainage and imbibition simulations that yield a *priori* predictions of the grain-scale configurations of water/ oil interface (menisci) within the fractionally wetted porous medium.

We used this grain based and mechanistic model to predict macroscopic properties (e.g. *P-S* curve for imbibition and drainage) of fractionally wetted porous medium that is qualitatively in agreement with experimental data. The experimental data and simulation result show a non-linear behavior between the position of *P-S* curves and fraction of oil-wet grains.

This grain based approach captures the key pore-level events that govern drainage and imbibition in fractionally wet media. It thus allows mechanistic, *a priori* predictions of displacement behavior such as capillary pressure curves for these materials that cannot be obtained from traditional pore network models.

Acknowledgements

SM expresses his thanks to Dr. Masa Prodanovic and Joanna L. Castillo for helpful discussion and preparing some of figures. Partial support for SM came from the US Dept. of Energy, grant # DE-FC26-04NT15518.

References

Al-Futaisia, A., Patzek, T. W. 2004. Secondary imbibition in NAPL-invaded mixed-wet sediments. *J. Contaminant Hydrology* **74**: 61– 81.

Anderson, W. G. 1987a. Wettability Literature Survey.4. Effects of wettability on capillary-pressure. *J. Pet. Tech.* **39** (10): 1283-1300.

Anderson, W. G. 1987b. Wettability Literature Survey.4. Effects of wettability on relative permeability. *J. Pet. Tech.* **39** (11): 1453-1468.

Bauters, T.W.J., Steenhuisa, T.S., DiCarlo, D.A., Nieberc, J.L., Dekkerd, L.W., Ritsemad, C.J., Parlangea, J.-Y., Haverkampe, R. 2000. Physics of water repellent soils. *J. Hydrology* **231:** 233–243.

Blunt, M.J., 1998. Physically based network modeling of multiphase flow in intermediate-wet porous media. *J. Pet. Sci. Eng.* **20**: 117– 125.

Bradford, S. A., Leij, F. J. 1995. Fractional wettability effects on two-and three-fluid capillary pressure-saturation relations. *J. Contaminant Hydrology* **20:** 89-109.

Brown. , R. J. S. and Fatt, I. 1956. Measurements of Fractional Wettability of Oil Fields Rocks by the Nuclear Magnetic Relaxation Method. SPE 743 presented at fall meeting of the Petroleum Branch of AIME, Los Angeles , 14-17 October.

Dullien, F. A. L. 1992. *Porous Media; Fluid Transport and Pore Structure*, second edition, San Diego, California: Academic Press.

Gladkikh, M., and Bryant, S. 2005. Prediction of imbibition in unconsolidated granular materials, *Journal of Colloid and Interface Science* **288:** 526-539.

Haines, W.B. 1927. Studies in the physical properties of soils. IV. A further contribution to the theory of capillary phenomena in soil. *J Agric Sci* **17:** 264 – 290.

Han, J., N Jin, Y. and Willson, C. 2006. Virus Retention and Transport in Chemically Heterogeneous Porous Media under Saturated and Unsaturated Flow Conditions. *Environ. Sci. Technol*. **40**: 1547-1555.

Heiba, A. A., Davis, H. T., and Scriven, L. E. 1983. Effect of Wettability on Two-Phase Relative Permeabilities and Capillary Pressures. *SPE* 12172 presented at SPE Annual Technical Conference and Exhibition, San Francisco, 5-8 October.

Laroche, C., Vizika, O., and Kalaydjian, F. 1999. Network modeling as a tool to predict three-phase gas injection in heterogeneous wettability porous media. *J. Pet. Sci. Eng*. **24**: 155– 168.

McDougall, S. R., and Sorbie, K. S. 1993. The Prediction of Waterflood Performance in Mixed-Wet Systems From Pore-Scale Modeling and Simulation. SPE 25271 presented at SPE Symposium on Reservoir Simulation, New Orleans, 28 February - 3 March.

Melrose, J.C. 1965. Wettability as related to capillary action in porous media. *SPEJ* **5:** 259 – 271.

Mohanty, K. K., Salter, S. J. 1983. Multiphase flow in Porous Media: III. Oil Mobilization, Transverse Dispersion, and Wettability. SPE 12127 presented at SPE Annual Technical Conference and Exhibition San Francisco, 5-8 October.

Morrow, N. R. 1990. Wettability and its Effects on Oil Recovery. *JPT* **42:** 1476; *Trans., AIME* **289**.

Piri, M., and Blunt, M. J. 2002. Pore-scale modeling of three-phase flow in mixed-wet systems. SPE 77726 presented at SPE Annual Technical Conference and Exhibition, San Antonio, 29 September-2 October.

Salathiel, R. A. 1973. Oil Recovery by Surface Film Drainage in Mixed-Wettability Rocks, *J. Pet, and Tech.:* 1216-1224; *Trans: AIME*, 155.

Sharma, M.M., Garough, A., Dunlap, H.F., 1991. Effects of wettability, pore geometry and stress on electrical conduction in fluid saturated rocks. *Log Analyst* **32**: 511–526.

Skjaeveland, S.M., Siqveland, L.M., Kjosavik, A., Hammervold Thomas, W.L., Virnovsky, G.A. 2000. Capillary Pressure Correlation for Mixed-Wet Reservoirs. *SPE Reservoir Eval. & Eng.* **3**(1): 60-67.

Tsakiroglou a, C. D., Fleury, M. 1999. Resistivity index of fractional wettability porous media. *J. Pet. Sci. Eng*. **22**: 253– 274.

Ustohal, P., Stauffer, F., Dracos, T. 1998. "Measurement and modeling of hydraulic characteristics of unsaturated porous media with mixed wettability. *J. Cont. Hydrology* **33:** 5-37.

Valvatne, P. H., and Blunt, M. J. 2004. Predictive pore-scale modeling of two-phase flow in mixed wet media, *Water Resour. Res*. **40**, W07406.

Van Dijke, M.I.J., Sorbie, K.S., McDougall, S.R. 2000. A Process-Based Approach for Three-Phase Capillary Pressure and Relative Permeability Relationships in Mixed-Wet Systems. *SPE* 59310 presented at SPE/DOE Improved Oil Recovery Symposium, Tulsa, 3–5 April.

Table 1—Bubbling pressure (Pb) and Corey exponent (λ) for the measured 0% and 100% oil-wet imbibition curves. For fractionally-wet sands, the only parameter that was fit was α, the fraction of the 0% curve needed to fit the data.

Media	Pb (Pa)	λ	α
0% oil-wet	1050	4	1.0
25% oil-wet			0.85
50% oil-wet			0.49
75% oil-wet			0.10
100% oil-wet	-1900	15	0.0

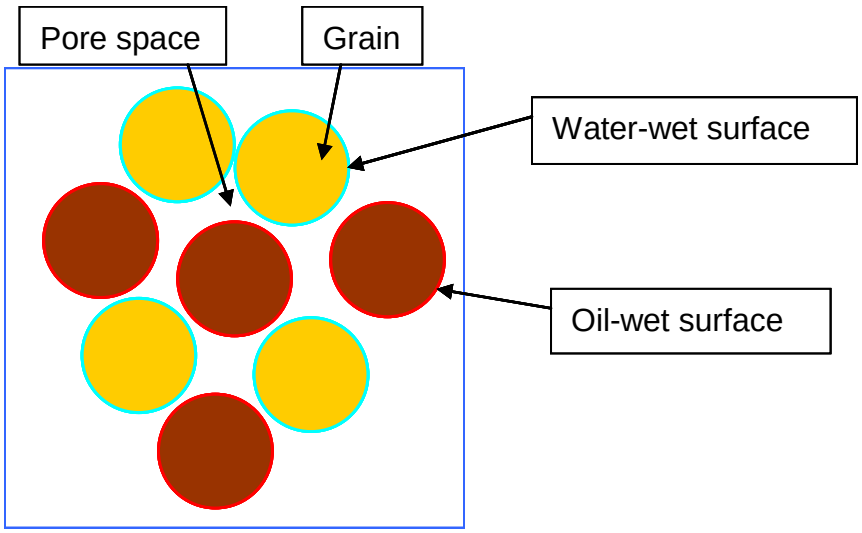

Fig. 1. Schematic of fractional wetted porous media (grain level scale)

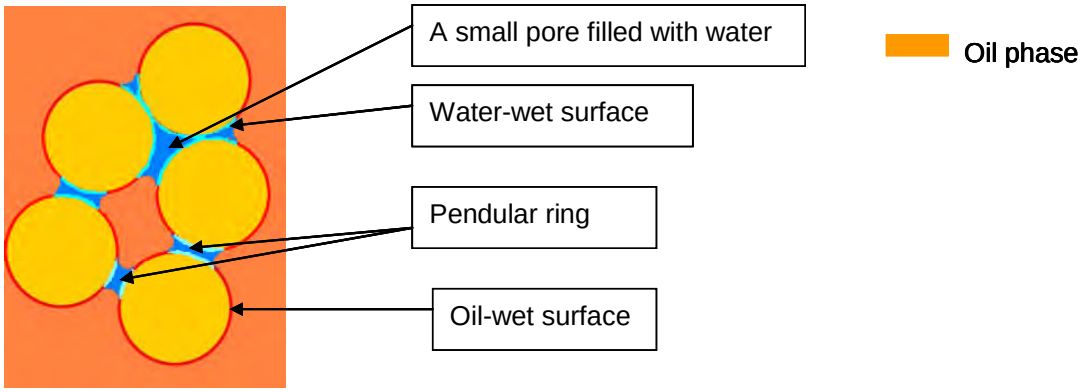

Fig. 2. Schematic of mixed wetted porous media (grain level scale)

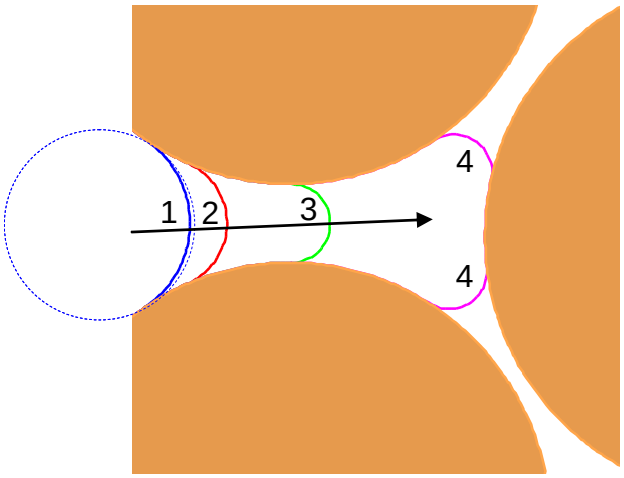

Fig. 3. Schematic of a pore filling under the Haines criterion. Originally the meniscus is located in the left hand throat (blue curve, location 1). The meniscus is an arc of a circle whose radius is set by the applied capillary pressure. Increasing the curvature causes the circle to become smaller, until it can pass through smallest opening of the throat (green curve, location 3). The green curve is unstable and the pore will be drain and results in locating two menisci at adjacent throats (purple curves, location 4).

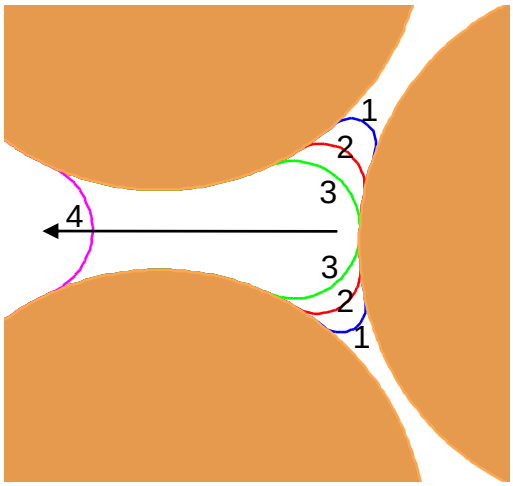

Fig. 4. Schematic of a pore filling under the Melrose criterion. Two menisci are originally located at two adjacent throats (blue curve, location 1); by decreasing curvature (capillary pressure), menisci move toward the pore. Different color curve shows the position of menisci at different curvature. Eventually these two menisci touch each other (green curve, location 3), the green curve is unstable and pore will be imbibed by wetting phase. The merged meniscus jumps to a new stable location, the purple curve (location 4).

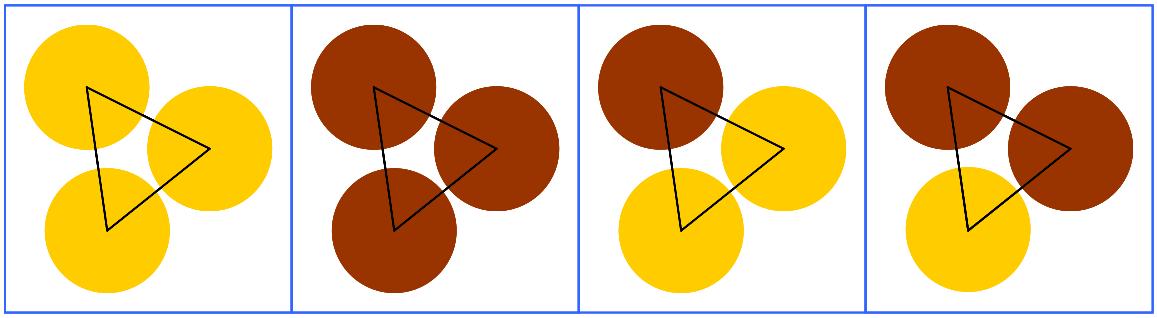

Fig. 5. Schematic of different configurations of a pore in the fractionally wetted porous media. The throat is the void space (gap) within two pair of disks. In configuration a, and b the throats are uniformly wetted, whereas in configurations c and d two of throats are fractionally wetted and one of them are uniformly wetted.

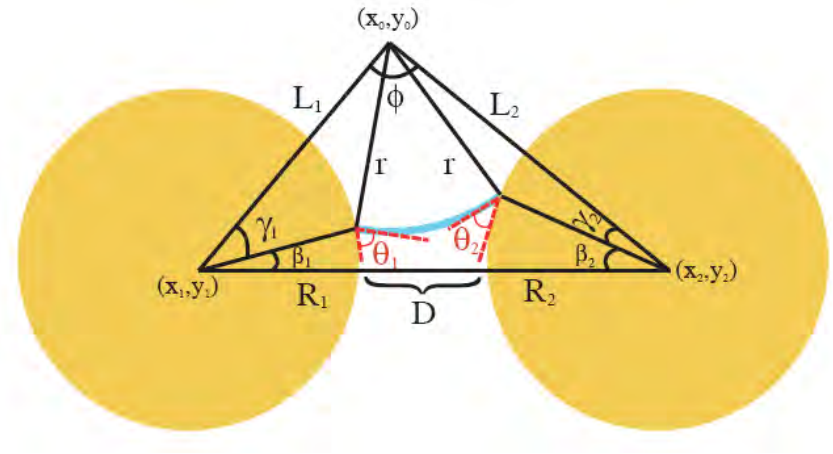

Fig. 6. The schematic of a stable meniscus (blue) with a radii curvature of r, located on two disks with different contact angle (θ_1,θ_2). The disks can have different radii (R_1,R_2).

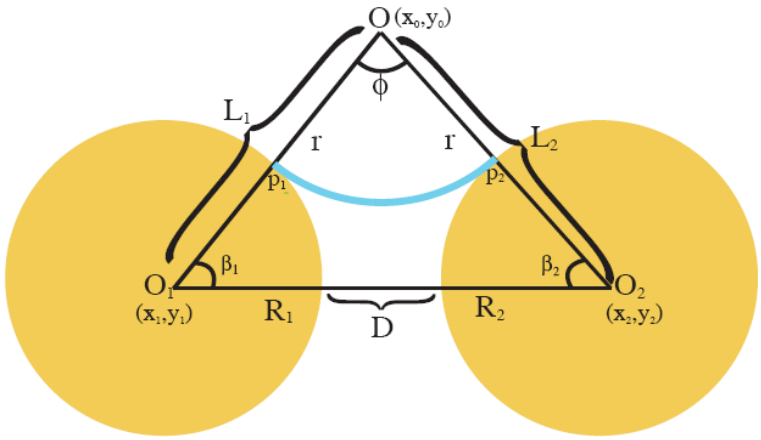

Fig. 7. The schematic of menisci (blue) with radii curvature of r, located on two disks with zero contact angles ($\theta_1=\theta_2=0$). The disks have same radius ($R_1=R_2=R$) and are separated by a gap of width D.

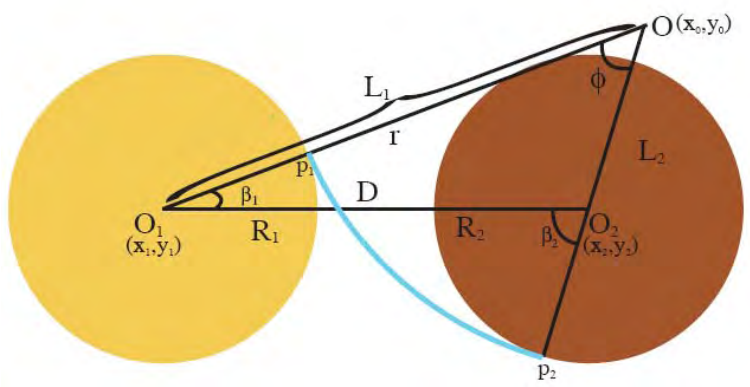

Fig. 8. The schematic of menisci (blue) with radii curvature of r, located on two disks with zero and 180° contact angles ($\theta_1=0$, $\theta_2=180^o$). The disks have same radius ($R_1=R_2=R$)

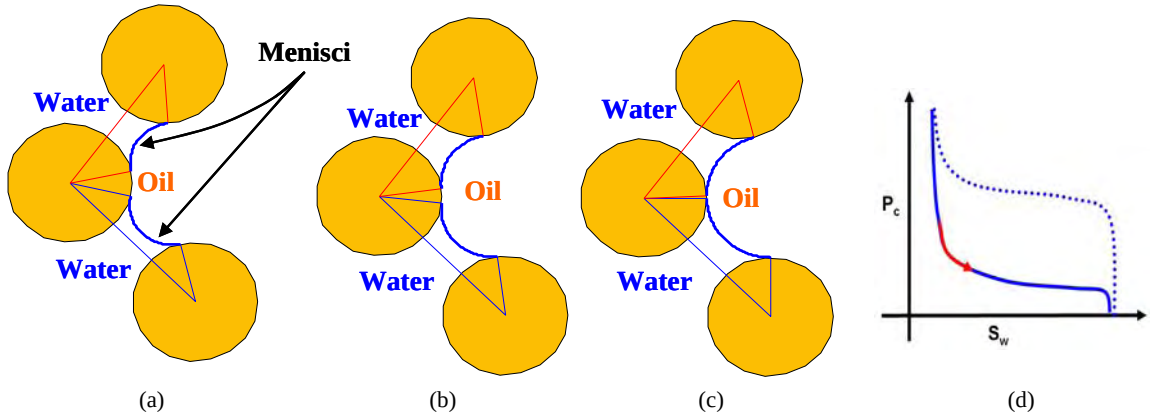

Fig. 9. Schematic of merging two menisci (Melrose event) in uniformly wetted porous medium. Three water wet disks construct a pore and three throats, and originally the two menisci are located on the two adjacent throats (a). The menisci move toward the pore by decreasing curvature (b), until they touch (c) and the pore fills with water. This Melrose event happens during imbibition as the curvature is decreased (d).

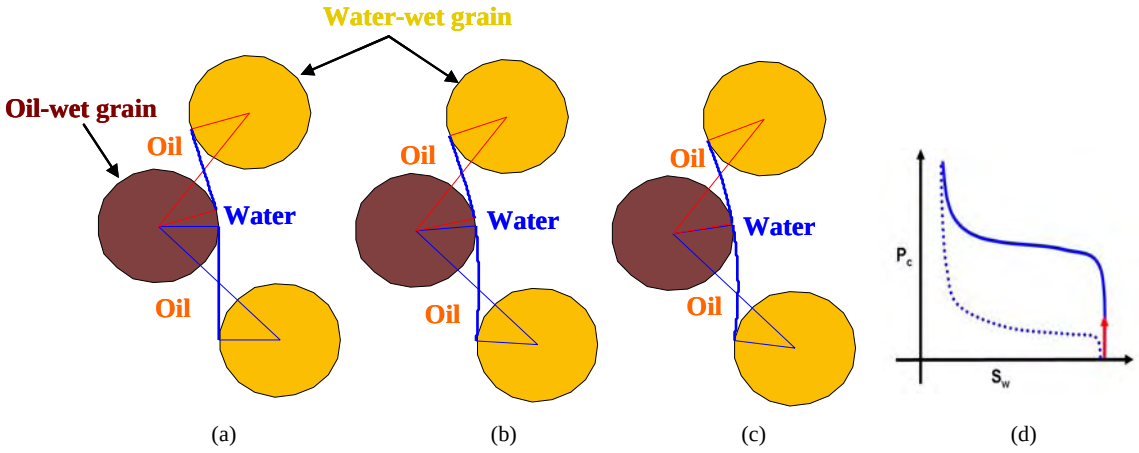

Fig. 10. Schematic of merging two menisci (Melrose event) in fractionally wetted porous medium, two water wet disks and one oil wet disk construct a pore and three throats where two of them are fractionally wetted and one is uniformly wetted. Originally two menisci located on the two adjacent throats which are fractionally wetted (a). The menisci move toward the pore by increasing curvature (b), until they touch (c) and the pore fills with oil. This Melrose event happens during drainage as the curvature is increased (d).

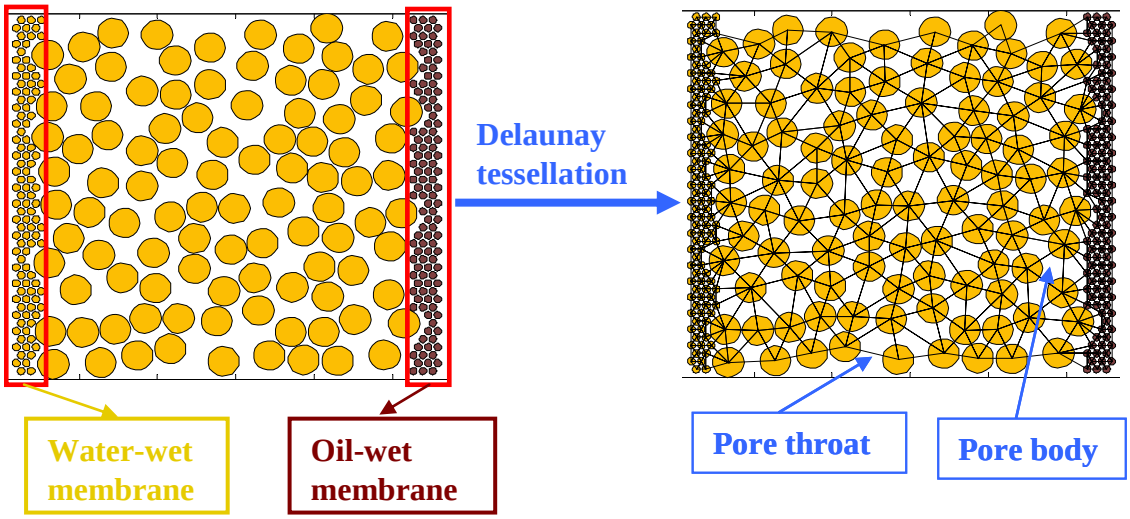

Fig. 11. (a) Schematic of porous medium made from randomly distributed disks, the oil wet membrane and water wet membrane located at left and right hand side of porous medium. (b) Schematic of network model extracted from porous medium (Fig. 9a). The pore space within porous medium can be divided to pore bodies and pore throats using Delaunay tessellation.

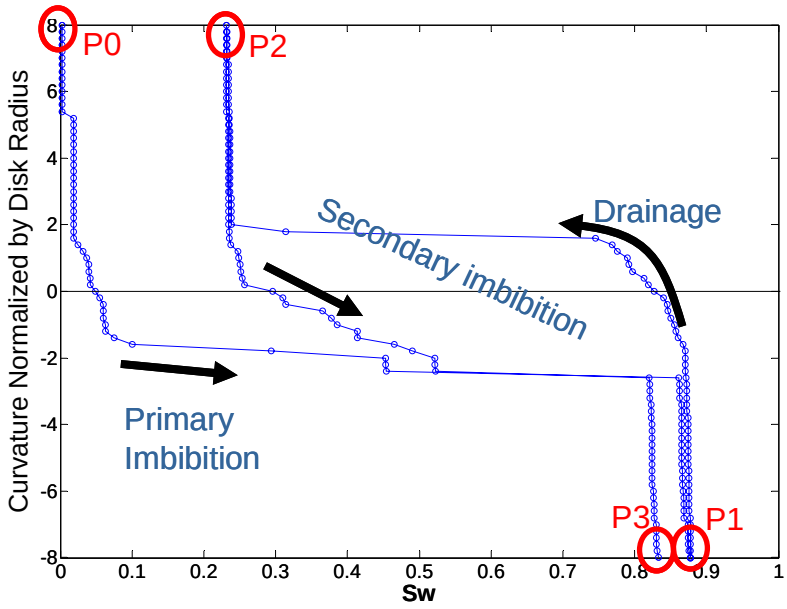

Fig. 12. The imbibition and drainage curves for a porous medium with 50 % of disks are oil-wet. The porous medium was filled with oil phase initially: first water phase push the oil out by decreasing capillary pressure (primary imbibition), second the oil phase drained the water out of the porous medium by increasing capillary pressure (drainage), and finally water phase push in to the porous medium and replace the oil phase (secondary imbibition). In all of three curves presented in this figure, the curvature range from positive to negative value and it cross over the zero curvature. All of these three curves produced from the same code, the difference is just starting and ending applied curvature.

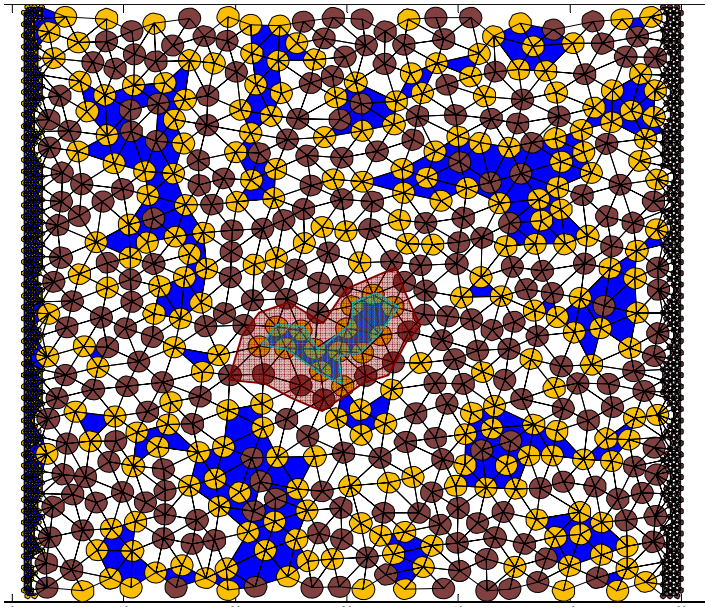

Fig. 13. The schematic of drainage end point for the porous medium with 50 % of disks are oil-wet (the same porous medium as Fig 9). The blue color represent trap water phase and the white color is oil phase. The dark brown disks are oil wet disks and the light brown disks are water wet disks. The region outlined in cyan shows a shell of water-wet grains in which a blob of water phase is trapped, the region outlined in dark red shows an outer shell of oil-wet grains around the water-wet shell. This pattern is characteristic of trapped water in this class of porous media.

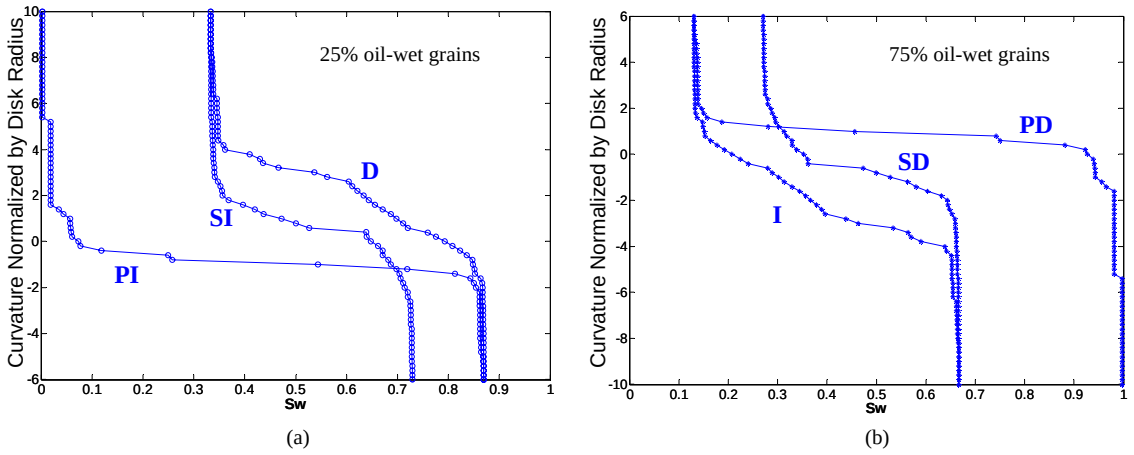

Fig. 14. (a) The primary (PI), drainage (D) and secondary imbibition (SI) curves for porous medium with 25% oil wet disks. (b) The primary, secondary imbibition and drainage curves for porous medium with 75% oil wet disks. The curves on the Figs. 12a and 12b are vertically symmetric, so if the Fig. 12b rotates 180°, the curve will be match with curves on Fig. 12a.

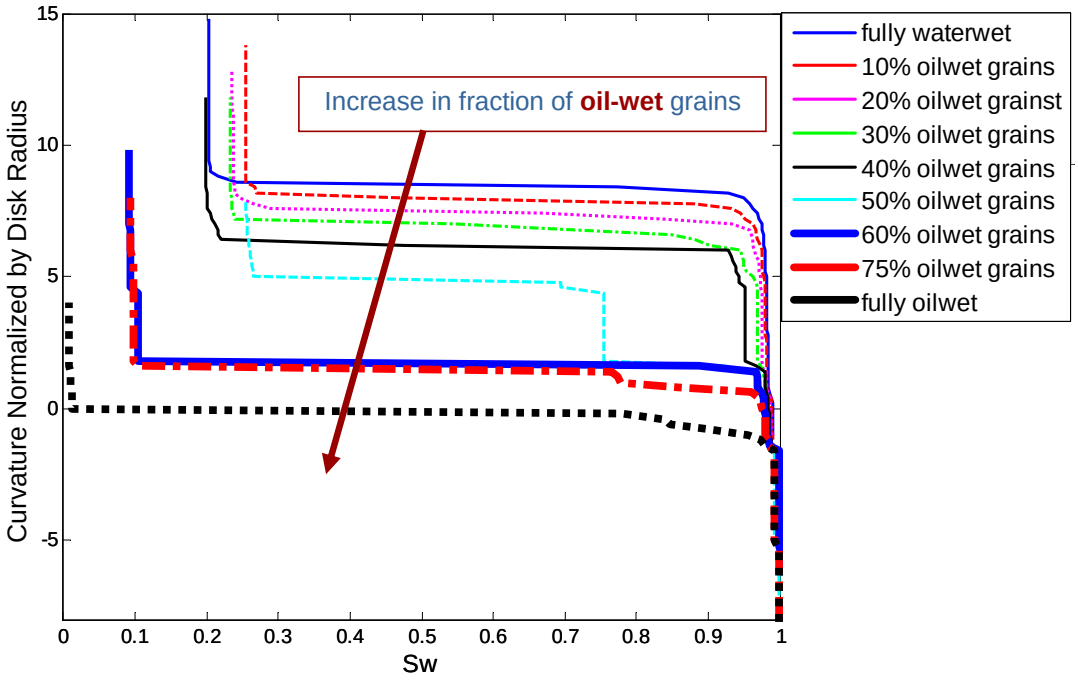

Fig. 15. Comparison between primary drainage curves for porous media with different fraction of oil-wet ($\theta_{ow} = 180°$) disks distributed randomly among water-wet ($\theta_{ww} = 0°$) disks. The porous media was originally filled with water. The oil phase pushes the water phase out as the capillary pressure (curvature) increases. As the fraction of oil-wet disks within porous medium increases the curvature which oil phase percolate through porous medium decreases.

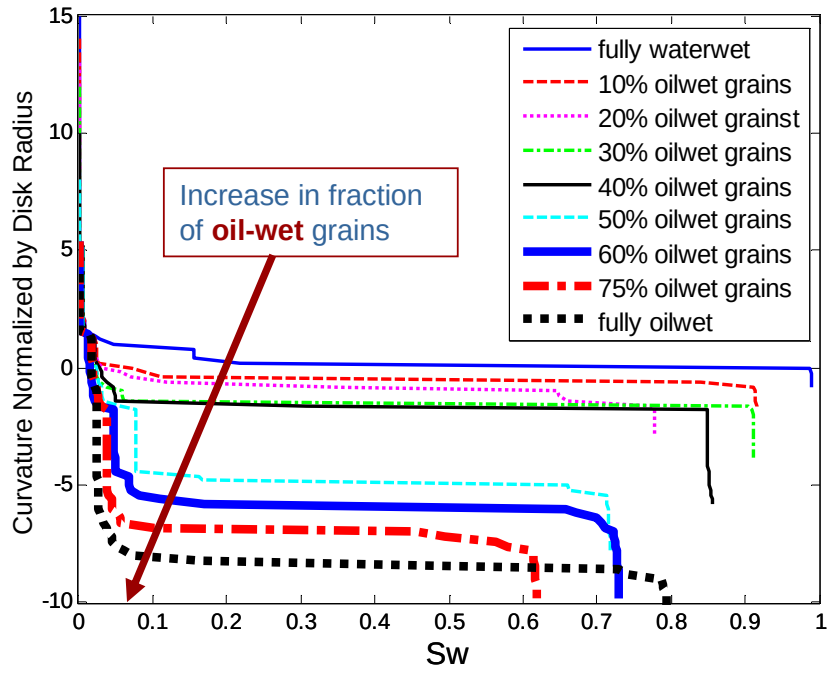

Fig. 16. Comparison between primary imbibition curves for porous media with different fraction of oil-wet disks; the contact angles on water-wet and oil-wet disks are $\theta_{ww} = 0°$ and $\theta_{ow} = 180°$, respectively. The porous media was originally filled with oil. The water phase pushes the oil phase out as the capillary pressure (curvature) decreases. As the fraction of oil-wet disks within porous medium increases the value for curvature which water phase percolate through porous medium decreases.

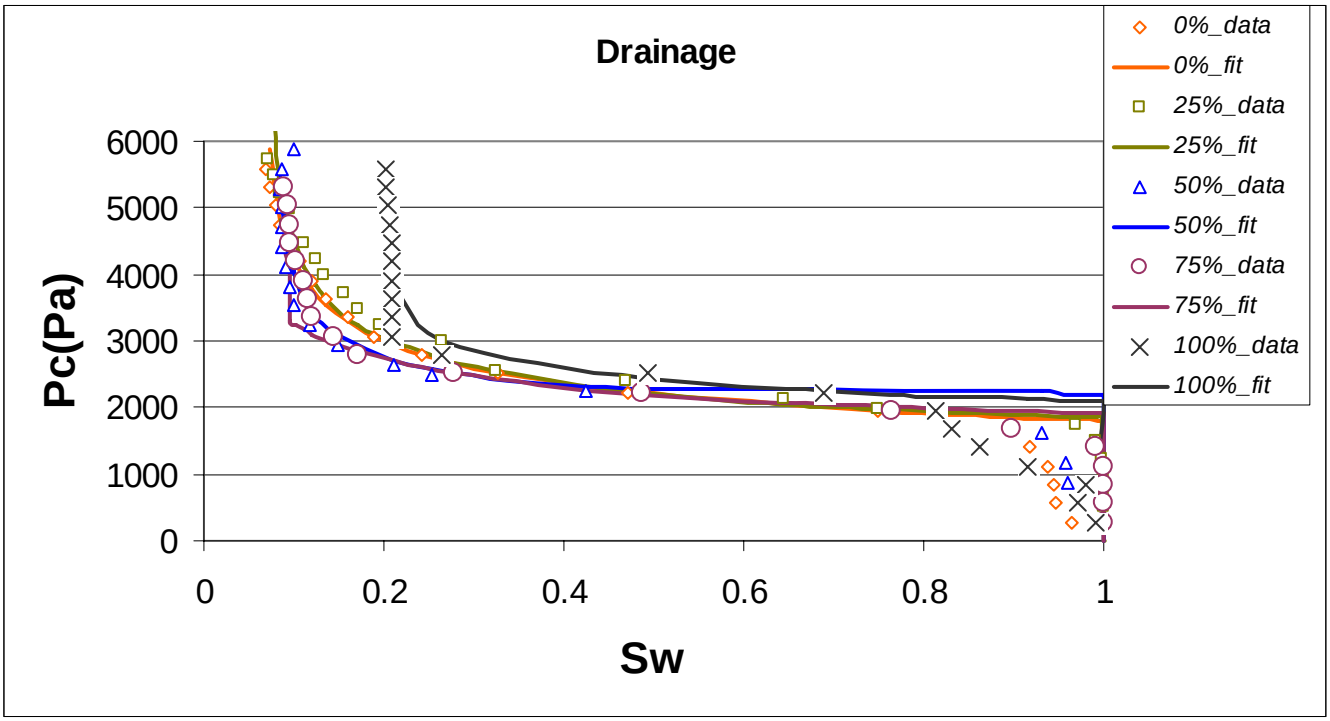

Fig. 17. Water/air drainage curves for fractionally-wet media. The drainage curves do not show much change with changing oil-wet fraction.

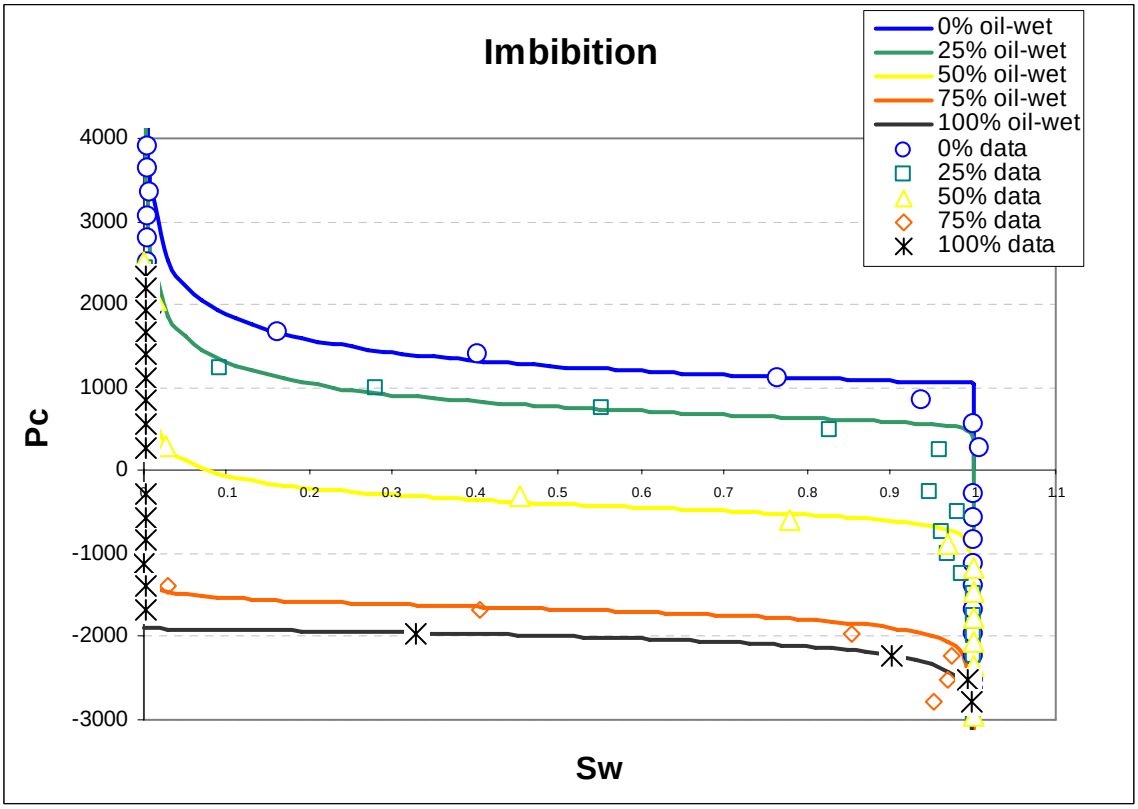

Fig. 18. Measured water/air imbibition curves for fractionally-wet media. The imbibition curves move monotonically lower with increasing oil-wet fraction.

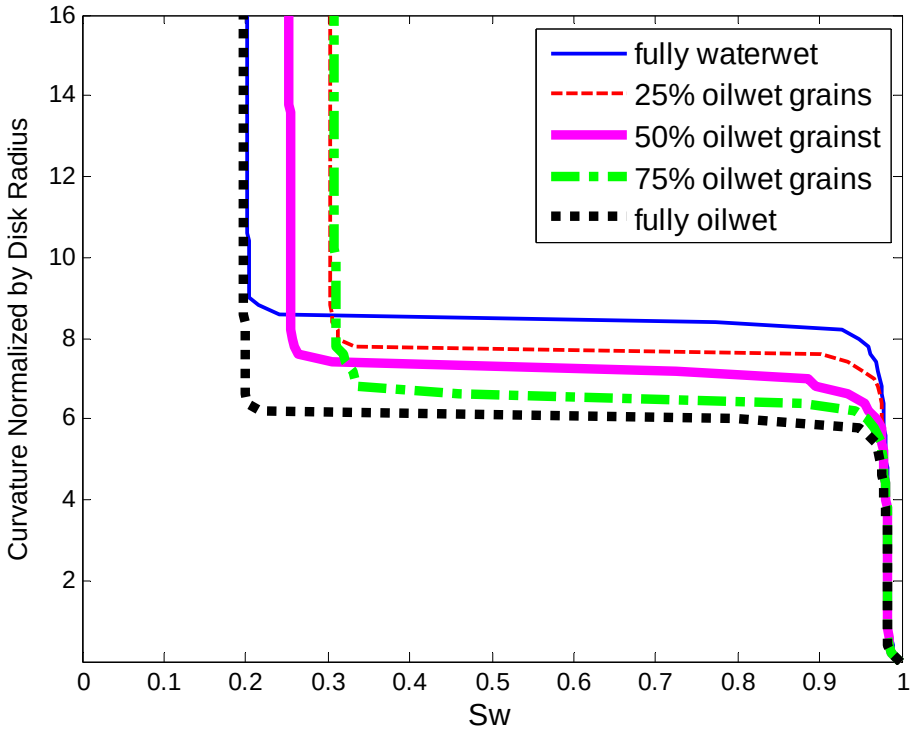

Fig. 19. Comparison between primary drainage curves for porous media with different fraction of oil-wet ($\theta_{ow} = 50°$) disks distributed randomly among water-wet ($\theta_{ww} = 0°$) disks. If the oil-wet disks are not perfectly hydrophobic, as commonly occurs in experiments when the grains are treated chemically, change in capillary pressure curve is less dramatic.